

1  
2  
3  
4  
5  
6  
7  
8  
9  
10  
11  
12  
13  
14  
15  
16  
17  
18  
19  
20  
21  
22  
23

*Geophysical Research Letters*

Supporting Information for

**Sub-cloud turbulence explains cloud-base updrafts for shallow cumulus ensembles: First observational evidence**

Youtong Zheng<sup>1</sup>, Daniel Rosenfeld<sup>2</sup>, and Zhanqing Li<sup>1</sup>

**Affiliations:**

<sup>1</sup>Earth System Science Interdisciplinary Center, University of Maryland, College Park, Maryland, 20742, USA.

<sup>2</sup>Institute of Earth Science, Hebrew University of Jerusalem, Jerusalem, Israel.

**Contents of this file**

1. Text S1~S2
2. Figures S1~S4
3. Table S1

24

25 **Text S1: LASSO data**

26 The Large-Eddy Simulation (LES) Atmospheric Radiation Measurements (ARM) Symbiotic  
27 Simulation and Observation (LASSO) project was launched in 2015 by the U.S. Department of  
28 Energy's ASR program (Gustafson Jr et al., 2020). Routine large-eddy simulations of shallow  
29 convection at ARM's SGP observatory were conducted between 2015 and 2019. One of the core  
30 concepts of LASSO is to provide a library of ShCu cases for researchers to conduct composite  
31 analysis with statistical robustness. This contrasts with previous LES studies that are limited to  
32 only a couple of ShCu cases. In this study, we use all the 18 ShCu cases released in the first two  
33 phases (2015 and 2016) of the LASSO. The output from two different models are used: Weather  
34 Research and Forecasting (WRF) (Skamarock et al., 2008) and System for Atmospheric Modeling  
35 (SAM) (Khairoutdinov and Randall, 2003). Both models were run with resolutions of 100 m in  
36 the horizontal and 30 m in the vertical within a domain with a size of 14.4 km. The initial state and  
37 the forcing data are the same: balloon-based sounding used as the initial state, large-scale-forcing  
38 input obtained from the European Centre for Medium-Range Weather Forecasts (ECMWF)  
39 analysis averaged over the spatial scale of 114 km, and the homogenized surface fluxes obtained  
40 from the ARM Variational Analysis (VARANAL) product. The WRF model used in this study  
41 adopted LASSO-Morrison cloud microphysical scheme (Gustafson et al., 2017) whereas the SAM  
42 uses the two-moment Bulk scheme (Morrison et al., 2005). Here, we offer additional discussions  
43 on two aspects of the LASSO data. First, one may suspect if the horizontal resolution of 100 m is  
44 fine enough for studying the vertical velocity (Guo et al., 2008; Donner et al., 2016; Endo et al.,  
45 2019). Since this study is focused on the ensemble-averaged vertical velocity, this resolution issue  
46 is more or less alleviated. Improving the horizontal resolution to 25 m has a discernable, but not  
47 significant, influence on the domain-averaged vertical velocity statistics (Endo et al., 2019).  
48 Second, the selection of the specific combinations of large-scale and surface forcing data is purely  
49 random. There is no conclusive evidence as to which combination of forcing is superior to others.

50 We determine the cloud-base height ( $z_b$ ) as the altitude with the largest cloud cover. At the  $z_b$ ,  
51 we selected cloudy pixels with liquid water greater than  $0.01 \text{ g m}^{-3}$  to compute the cloud-base  
52 updrafts. The averaging routines are the same as those described in Section 3 of the main  
53 manuscript. The  $\text{TKE}_{\text{ML}}$  is computed as  $0.5 * (u'^2 + v'^2 + w'^2)$  averaged below the  $z_b$ . The

54 mixed-layer height,  $h$ , is determined as the altitude with the most negative buoyancy fluxes. The  
55 convective time scale,  $t^*$ , is computed as  $h / (\text{TKE}_{\text{ML}})^{1/2}$ .

56

## 57 **Text S2: Comparison between the DL- and LAASO-derived results**

58 As shown in Figure 3a and S4c, d and summarized in Table S1, WRF and SAM show ~ 50%  
59 steeper slope of the relationships between the  $\overline{w_b}$  and  $(\text{TKE}_{\text{M}}^w)^{1/2}$  than that from the DL. We think  
60 that the larger slope is likely due to the known problem of LES in overestimating the updrafts near  
61 cloud bases (Endo et al., 2019). As shown in Endo et al., (2019), compared with DL observations,  
62 the LES tends to shift the probability density function (PDF) of cloud-base vertical velocities  
63 toward the positive end. This leads to weaker downdrafts and stronger updrafts at cloud bases.  
64 This problem is found to be a consequence of model physics underestimating the evaporative and  
65 radiative cooling near cloud bases, processes driving downdrafts. It's reasonable to conjecture that  
66 such an effect should be less influential for weaker sub-cloud forcing. As a thought experiment,  
67 one may imagine the evaporative cooling to approach zero as the convection gradually shuts off,  
68 leaving little chance for the underestimated evaporative cooling to modify the  $\overline{w_b}$ .

69

70

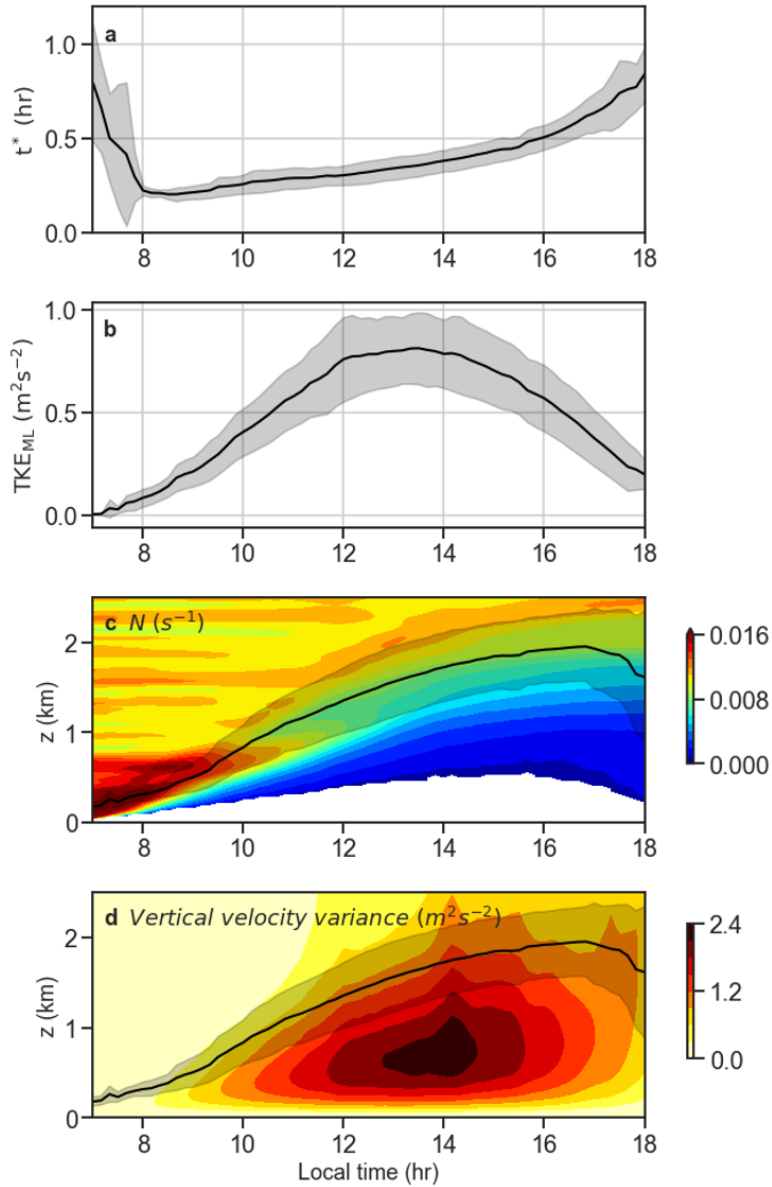
71

72

73

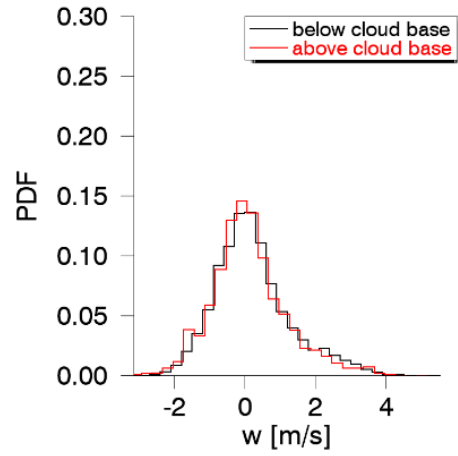
74

75



76

77 **Figure S1:** WRF-simulated composite diurnal variations of  $t^*$  (a),  $TKE_{ML}$  (b), and height-time  
 78 plots of Brunt-Vaisala frequency (c), and vertical velocity variance (d). In (c) and (d), the black  
 79 lines mark the diagnosed mixed-layer height ( $h$ ). All plotted are the composite means of the 18  
 80 ShCu cases from the 1<sup>st</sup> phase of the LAASO project.



81

82

**Figure S2:** Probability density functions of vertical velocity for pixels at 100 m below  
(black) and above (red) the cloud bases.

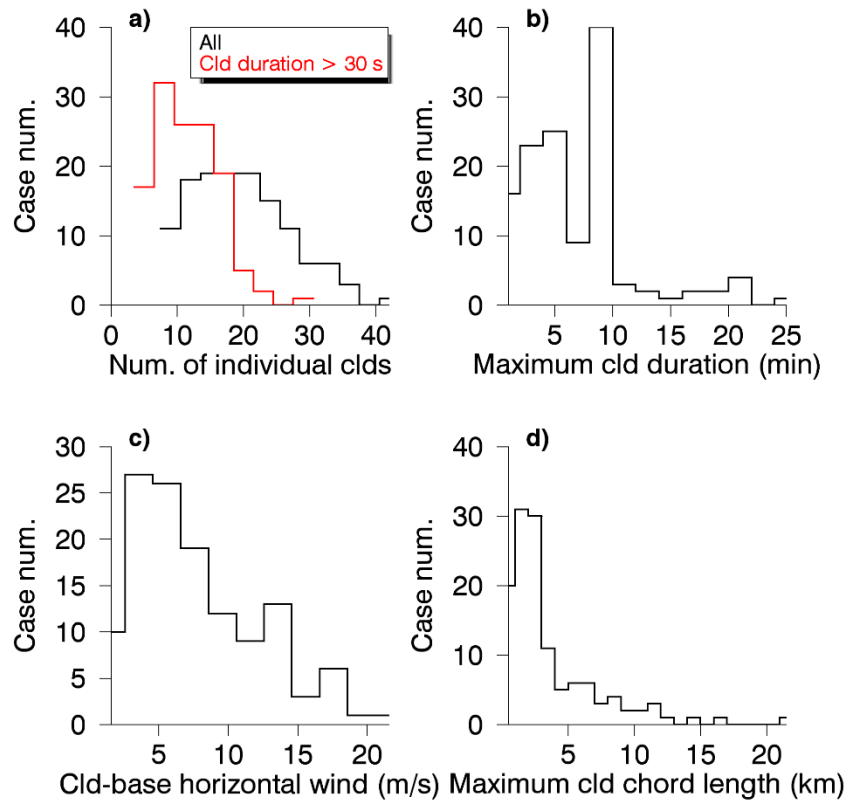
83

84

85

86

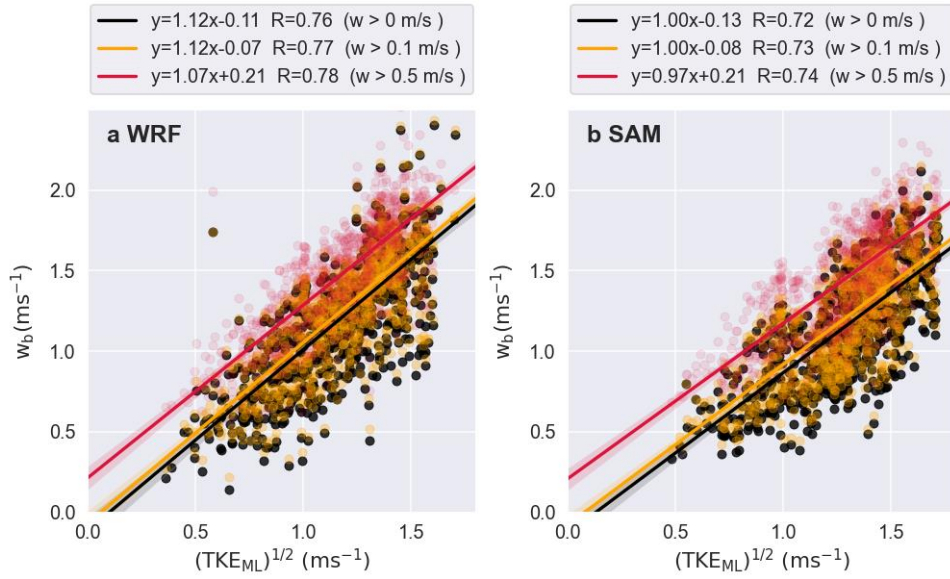
87



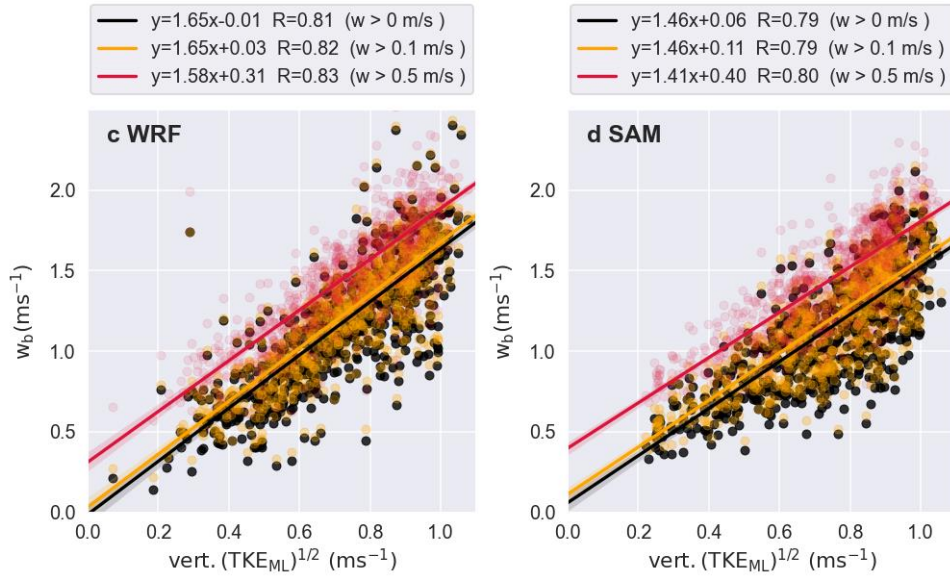
88

89 **Figure S3:** Statistical distribution of key quantities for the 128 ShCu cases including (a) the  
 90 number of individual cumuli (the red marks those that last longer than 30 secs), (b) maximum  
 91 cloud duration, (c) horizontal wind speed near cloud base, and (d) maximum cloud chord length.

92



93



94

95

**Figure S4:** Scatter plots of simulated  $\overline{w_b}$  versus  $(TKE_{ML})^{1/2}$  (upper) and  $(TKE_{ML}^w)^{1/2}$  (bottom), simulated by WRF (left) and SAM (right).

96

97

98

99

100

	Slope	Intercept (m/s)	Slope (forced through origin)	Corr.
DL $\overline{w_b}$ ( $w > 0$ m/s)	$1.04 \pm 0.09$	$0.11 \pm 0.06$	1.20	0.73
DL $\overline{w_b}$ ( $w > 0.1$ m/s)	$1.04 \pm 0.09$	$0.20 \pm 0.06$	N/A	0.73
DL $\overline{w_b}$ ( $w > 0.5$ m/s)	$0.98 \pm 0.10$	$0.61 \pm 0.07$	N/A	0.68
DL $\overline{w_b^{vol}}$ ( $w > 0$ m/s)	$1.81 \pm 0.15$	$0.22 \pm 0.10$	2.11	0.74
DL $\overline{w_b^{vol}}$ ( $w > 0.1$ m/s)	$1.80 \pm 0.15$	$0.24 \pm 0.10$	N/A	0.74
DL $\overline{w_b^{vol}}$ ( $w > 0.5$ m/s)	$1.64 \pm 0.14$	$0.50 \pm 0.10$	N/A	0.71
WRF $\overline{w_b}$ ( $w > 0$ m/s)	$1.65 \pm 0.04$	$-0.04 \pm 0.03$	1.63	0.81
WRF $\overline{w_b}$ ( $w > 0.1$ m/s)	$1.65 \pm 0.04$	$0.03 \pm 0.03$	N/A	0.82
WRF $\overline{w_b}$ ( $w > 0.5$ m/s)	$1.58 \pm 0.04$	$0.31 \pm 0.03$	N/A	0.83
SAM $\overline{w_b}$ ( $w > 0$ m/s)	$1.46 \pm 0.04$	$0.06 \pm 0.03$	1.54	0.79
SAM $\overline{w_b}$ ( $w > 0.1$ m/s)	$1.46 \pm 0.04$	$0.11 \pm 0.03$	N/A	0.79
SAM $\overline{w_b}$ ( $w > 0.5$ m/s)	$1.41 \pm 0.04$	$0.40 \pm 0.03$	N/A	0.80

**Table S1:** Statistics of the relationships between the ensemble-mean cloud-base updrafts and  $(\text{TKE}_{\text{ML}}^w)^{1/2}$  derived from DL, WRF, and SAM data.

101  
102  
103  
104  
105  
106  
107  
108  
109  
110  
111  
112  
113  
114

115 **Reference:**

- 116 Donner, L. J., O'Brien, T. A., Rieger, D., Vogel, B., & Cooke, W. F. (2016). Are atmospheric  
117 updrafts a key to unlocking climate forcing and sensitivity? *Atmospheric Chemistry and*  
118 *Physics*, *16*(20), 12983-12992. <Go to ISI>://WOS:000386665800002
- 119 Endo, S., Zhang, D., Vogelmann, A. M., Kollias, P., Lamer, K., Oue, M., et al. (2019). Reconciling  
120 differences between large-eddy simulations and Doppler lidar observations of continental  
121 shallow cumulus cloud-base vertical velocity. *Geophysical Research Letters*, *46*(20),  
122 11539-11547.
- 123 Guo, H., Liu, Y., Daum, P. H., Senum, G. I., & Tao, W.-K. (2008). Characteristics of vertical  
124 velocity in marine stratocumulus: comparison of large eddy simulations with observations.  
125 *Environmental Research Letters*, *3*(4), 045020.
- 126 Gustafson Jr, W. I., Vogelmann, A. M., Li, Z., Cheng, X., Dumas, K. K., Endo, S., et al. (2020).  
127 The Large-Eddy Simulation (LES) Atmospheric Radiation Measurement (ARM)  
128 Symbiotic Simulation and Observation (LASSO) Activity for Continental Shallow  
129 Convection. *Bulletin of the American Meteorological Society*, *101*(4), E462-E479.
- 130 Gustafson, W. I., Vogelmann, A. M., Cheng, X., Endo, S., Krishna, B., Li, Z., et al. (2017).  
131 *Recommendations for the implementation of the LASSO workflow*. Retrieved from
- 132 Khairoutdinov, M. F., & Randall, D. A. (2003). Cloud resolving modeling of the ARM summer  
133 1997 IOP: Model formulation, results, uncertainties, and sensitivities. *Journal of the*  
134 *Atmospheric Sciences*, *60*(4), 607-625.
- 135 Morrison, H., Curry, J., & Khvorostyanov, V. (2005). A new double-moment microphysics  
136 parameterization for application in cloud and climate models. Part I: Description. *Journal*  
137 *of the Atmospheric Sciences*, *62*(6), 1665-1677.
- 138 Skamarock, W. C., Klemp, J. B., Dudhia, J., Gill, D. O., Barker, D. M., Duda, M. G., et al. (2008).  
139 *G.: A description of the Advanced Research WRF version 3*. Paper presented at the NCAR  
140 Tech. Note NCAR/TN-475+ STR.

141  
142